

Effect of particle size of waste brick powder on the properties of alkaline activated materials

J Brînduş-Simuţ¹, M Vyšvařil¹, P Bayer¹, M Keppert² and P Rovnaníková¹

¹ Faculty of Civil Engineering, Brno University of Technology, Veverí 331/95, Brno 602 00, Czech Republic

² Faculty of Civil Engineering, Czech Technical University, Thákurova 7/2077, Praha 166 29, Czech Republic

E-mail: rovnanikova.p@fce.vutbr.cz

Abstract. The properties of alkaline activated brick dust mixed with water glass with a silicate modulus (Ms) of 1.0 were studied in fresh mixtures as well as hardened products in connection with the particle size of the dust. The brick dust (ground waste brick) was separated into 5 fractions according to particle size. The influence of particle size on the rheological properties of the fresh mixtures was studied via measurements of the yield stress and viscosity. The flexural and compressive strengths of the hardened products were determined after storage under laboratory conditions for 7, 14 and 90 days; the influence of 7 days of curing at 65°C on strength was evaluated as well. The microstructure of the hardened products was studied by means of porosimetry and SEM.

1. Introduction

Bricks are produced by the burning of clay minerals. During this process, a certain amount of amorphous phases of aluminosilicates are formed. Amorphous phases are necessary for pozzolanic activity, i.e. the reaction of brick powder with an alkaline solution. Brick powder is waste material from the production of calibrated brick elements; it can be also obtained from the processing of demolition waste. The effects of different conditions for the alkali-activation of brick powder have been studied. Reig et al. [1] activated red clay brick waste using sodium hydroxide and sodium silicate solutions. They studied the effects of several variables, mainly concentration of NaOH, SiO₂/Na₂O ratio and water/binder ratio on the porosity, composition and morphology of reaction products. With the optimal composition and a curing temperature of 65°C, a compressive strength of 50 MPa was achieved. Robayo et al. [2] reported similar results. Komnitsas et al. [3] focused on the effects of the particle size of waste brick powder and the temperature of curing on the properties of hardened pastes. They studied the aging period, the temperature of curing and the effect of freeze-thaw cycles on compressive strengths. When studying the composition of the product, they found a new mineral phase, pirssonite. Sassoni et al. [4] designed a mixture of alkali-activated brick powder for use as a repair material for brick masonry. Molar ratios of SiO₂/Al₂O₃ ranging from 0.4 to 1.4 and curing temperatures of 20 and 50°C were investigated. Pastes with SiO₂/Al₂O₃ ratios of 0.8 and 0.9 exhibited open porosity and water vapour permeability fairly similar to those of historic lime-based mortars.

The surface area of the waste brick powder is an important factor in the course and outcome of the reaction. Different granulometric classes of calcined clay (125 µm, 100 µm, 80 µm and 63 µm) were used as an aluminosilicate precursor for the fabrication of geopolymers. The influence of particle size on the kinetics of geopolymerization reactions and on the mechanical properties of geopolymers



was studied [5]. As the particle size of the waste brick powder decreased, the rate of reaction increased.

The rheological properties of alkali-activated materials are different from those of Portland cement-based pastes [6–8]. The mechanisms of the formation of an aluminosilicate gel at an early age are strongly dependent on the chemical composition of the mixture, i.e. on the type of precursor and the composition of the activator. The presence of Ca in solid precursors, for example in slags or fly ashes, could dramatically change the chemistry of the system, and this will change the rheological properties of fresh pastes [9].

A precursor is a waste material that can vary in particle size. Therefore, the aim of the study was to monitor the effect of particle size on the properties of fresh mixtures and hardened products.

2. Materials and methodology

2.1 Characterization of raw materials

The investigated brick powder originates from the grinding of calibrated brick elements from the HELUZ Brickworks factory, v.o.s., located in Hevlín (Czech Republic). The chemical composition of the brick powder was obtained via XRF analysis (PANalytical) and is presented in Table 1; the mineralogical composition was obtained via XRD analysis (SAXS - PANalytical Empyrean) and is specified in Table 2. The proportions of the components were calculated via Rietveld analysis. Sodium water glass (Vodní sklo, a. s., Czech Republic) contains 26.43% SiO₂, 16.61% Na₂O, and 56.96% H₂O. The ratios of the elements contained in samples of alkali-activated brick powder are Si/Al = 0.44, Ca/Si = 0.23, (Na+K)/Si = 0.27, (Na+K)/Al = 0.12, (Na+K+Ca+Mg)/(Si+Al) = 0.17.

Table 1. Chemical composition of brick powder.

	SiO ₂	Al ₂ O ₃	Fe ₂ O ₃	CaO	MgO	K ₂ O	Na ₂ O	P ₂ O ₅	TiO ₂	SO ₃	Sum
Mass %	55.5	17.0	5.8	10.5	2.4	2.8	0.7	0.2	0.8	1.9	97.6

Table 2. Mineralogical composition of brick powder.

Mineral	Formula	[%]
Quartz	SiO ₂	26.2
Hematite	Fe ₂ O ₃	2.3
Albite	NaAlSi ₃ O ₈	13.0
Microcline	KAlSi ₃ O ₈	3.6
Orthoclase	KAlSi ₃ O ₈	3.5
Muscovite	KAl ₂ (AlSi ₃ O ₁₀)(OH) ₂	12.5
Illite	K _{0.65} Al ₂ (Al _{0.65} Si _{3.35} O ₁₀)(OH) ₂	3.8
Diopside	CaMgSi ₂ O ₆	4.4
Akermanite	Ca ₂ MgSi ₂ O ₇	2.8
Amorphous	-	27.8

The pozzolanic activity of the brick powder was determined using the modified Chapelle test. A mixture of freshly annealed lime and water in a tightly closed container is stirred with a magnetic stirrer at a temperature of 93°C for 24 h inside a thermobox. The residual calcium hydroxide is determined via the saccharide method. The result represents the amount of calcium hydroxide consumed in the reaction of 1 g of brick powder per 24 hours. The pozzolanic activity of the used brick powder is 356 mg Ca(OH)₂ per 1 gram of brick powder. Pozzolanic activity is an important parameter for the alkaline activation of brick powder.

The particle size distribution of the brick powder with grains of less than 1 mm in diameter is shown in Figure 1, where $d_{10} = 2.094 \mu\text{m}$, $d_{50} = 18.750 \mu\text{m}$, and $d_{90} = 302.256 \mu\text{m}$. The brick powder was sorted into 5 fractions: 0–90 μm , 0–125 μm , 0–250 μm , 0–500 μm and 0–1000 μm .

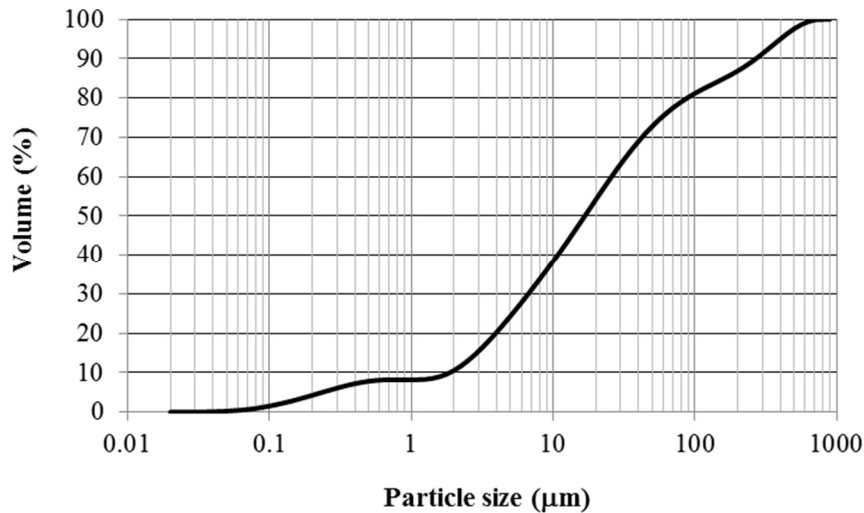


Figure 1. Particle size distribution of the brick powder.

2.2. Composition of tested mixtures

The mixtures containing alkali-activated brick powder were prepared from 200 g of brick powder of an appropriate particle size, and an alkaline solution which contains 44 g of sodium water glass with a silicate modulus (M_s) of 1.6, 6.04 g of sodium hydroxide, and 56 g of water. The total mass of the raw materials was kept constant for all samples, and the silicate modulus of the alkaline solution was $M_s = 1.0$ for all mixtures. Five mixtures with different brick powder particle sizes (Table 3) were prepared for subsequent testing. First, the alkaline activator was prepared by mixing sodium hydroxide solution with sodium water glass; second, the brick powder and alkaline activator were blended together.

Table 3. Particle size of brick powder in mixtures.

	G1	G2	G3	G4	G5
Grain size [mm]	0 – 0.09	0 – 0.125	0 – 0.250	0 – 0.500	0 – 1.000

The fresh mixtures were poured into moulds; they were then covered with PE foil and stored for 1 day in the laboratory at $20 \pm 1^\circ\text{C}$. After 1 day the test specimens were demoulded and wrapped in the PE foil again. Some of the specimens were stored at a laboratory temperature of $20 \pm 1^\circ\text{C}$ for 7, 28 and 90 days, while the remainder were stored at a temperature of 65°C for 7 days.

3. Experimental procedure

The flow properties and viscoelastic characteristics of the pastes were evaluated through rheological measurements with the aid of a Discovery HR-1 (TA Instruments) hybrid rheometer and TRIOS 4.0.2.30774 software. The measurements were performed in a Peltier Concentric Cylinder system with a DIN rotor at 25°C . The paste was introduced into the measurement system at the end of the mixing cycle. After a 60s period of rest, the rheological measurements were started. The testing routine comprised a shear rate increase (from 0.1 to 100 s^{-1}) applied in 30 steps with 15 s of measuring time at each shear rate. This was followed by a gradual reduction in the shear rate performed in the same manner. The results were expressed as shear rate vs. shear stress (flow curves) and the Herschel-Bulkley model (1) was applied to the descending branches of the flow curves in order to fit the experimental data. It was also used to describe the rheological behaviour of the pastes [10]:

$$\tau = \tau_0 + k\dot{\gamma}^n \quad (1)$$

where τ is the shear stress, $\dot{\gamma}$ is the shear rate, τ_0 corresponds to the yield stress, k is the consistency coefficient and n is the fluidity index which characterizes the shear-thinning ($n < 1$) or shear-thickening ($n > 1$) behaviour of the material. The time evolutions of the viscoelastic properties of the pastes were evaluated by small amplitude (0.01%) oscillation tests at 1 Hz frequency. These tests measured the dynamic moduli G' and G'' , which represent the elastic and viscous behaviour of the material. If the elastic behaviour is dominant ($G' > G''$), the sample exhibits the characteristics of a gel or solid state. Conversely, if $G'' > G'$, the sample shows the properties of a liquid.

The bending and compressive strengths of 20×20×100 mm test specimens were determined. Prior to the testing of their mechanical properties, the specimens were weighed and their dimensions measured. Bulk densities were calculated from the measured values. The porosity of the alkali-activated brick powder was assessed using a PoreSizer 9310 mercury porosimeter (Micromeritics). Pore diameter, cumulative intruded volume, cumulative pore surface and differential intruded volume were determined. Detailed microstructure images were taken via a MIRA3 XMU environmental scanning electron microscope (Tescan) [11, 12]. Three samples, designated G1, G2 and G3, were monitored.

4. Results and discussion

4.1. Rheological properties

The shape of the descending branches of the flow curves (Figure 2) indicates the dilatant character of the brick powder pastes. The yield stress of the pastes varied with the particle distribution in the brick powder (Table 4). With increasing particle sizes up to 0.25 mm the yield stress decreased, which was expected, but grew again with larger particles. The yield stresses of the pastes were very high and considerably higher than the yield stresses of metakaolin geopolymers [13]. The consistency coefficients of the pastes (Table 4) were on the same value level as for metakaolin geopolymer pastes [14], and they decreased with increasing brick powder particle size. This is due to the decrease in amorphous phase content as brick powder particle size increases. Mixtures with high crystalline content are very reluctant to flow. The fluidity indexes of pastes were higher than 1, which proved these mixes were shear-thickening. The shear-thickening character of the pastes became more significant with increasing brick powder particle size.

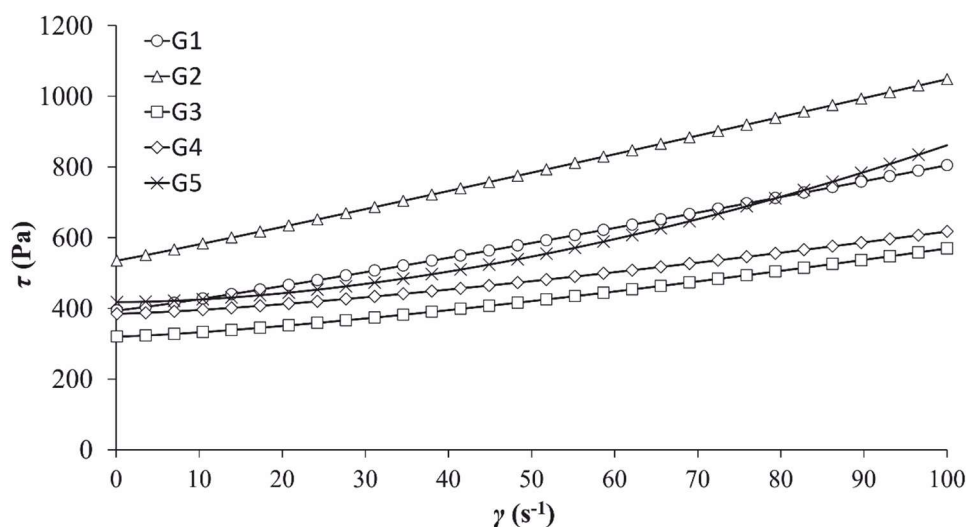


Figure 2. Descending branches of flow curves of brick powder mixtures.

Figure 3 shows the time evolution of the viscoelastic parameters G' and G'' during a small amplitude (0.01%) oscillation test. It is evident that G' decreased and G'' increased with increasing brick paste particle size. This means that with increasing particle size, the viscous component grows and the paste structure becomes less stiff, which is also displayed via the diminishing viscosity (consistency coefficient) of the pastes.

Table 4. Flow parameters of brick powder mixtures obtained from the Herschel-Bulkley model.

	τ_0 (Pa)	k (Pa s)	n (-)
G1	534.80	4.19	1.04
G2	393.70	2.54	1.10
G3	320.01	0.59	1.31
G4	384.65	0.50	1.33
G5	417.67	0.12	1.79

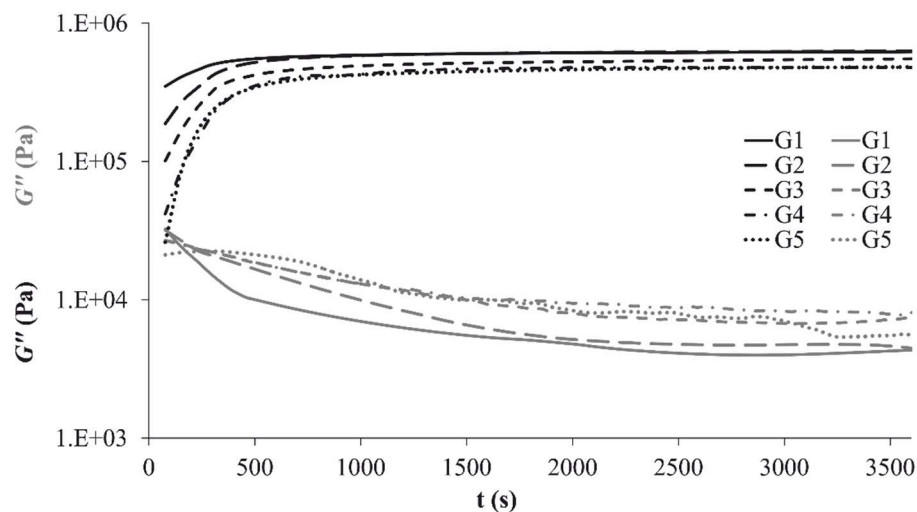


Figure 3. Time evolution of the storage modulus (G') and loss modulus (G'') of brick powder mixtures.

4.2. Mechanical properties

The bulk densities were independent of the time and temperature of curing. The specimens cured at 20°C had higher bulk densities (1860 to 1910 kg·m⁻³) compared to the specimens cured at a temperature of 65°C for 7 days (1720 to 1820 kg·m⁻³).

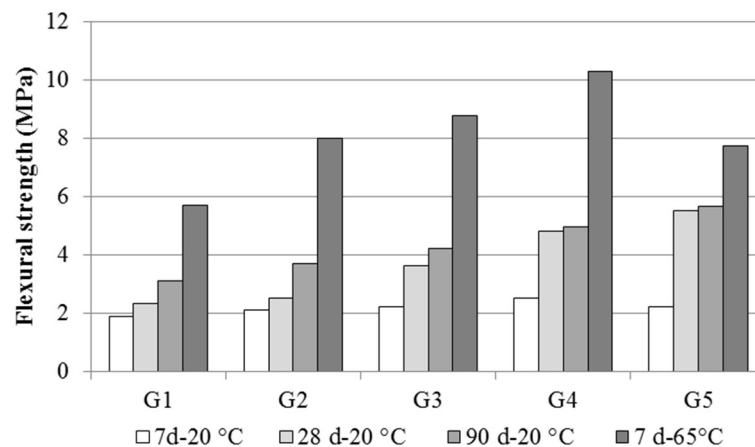


Figure 4. Flexural strength over time.

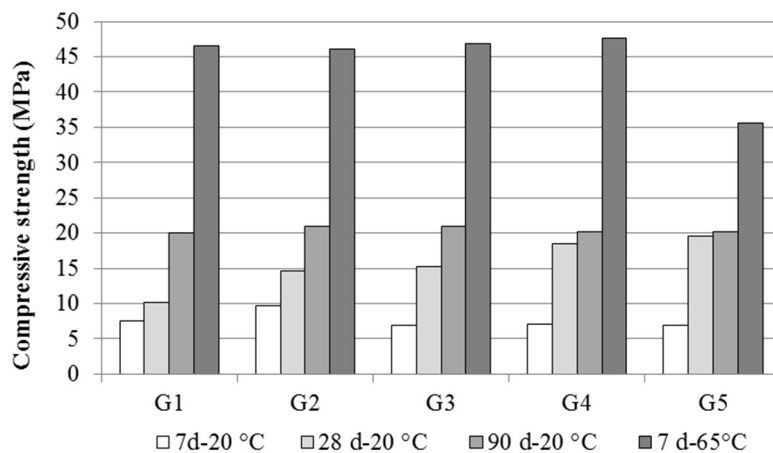


Figure 5. Compressive strength over time.

The flexural strengths (Figure 4) of pastes increased with curing time at 20°C, and with larger brick grain size. Significantly higher strengths reached specimens cured at 65°C. Compressive strength (Figure 5) also increased with time of curing up to 28 days, but in contrast to flexural strength all samples exhibit approximately similar compressive strengths at 90 days. The compressive strength of specimens cured at 65°C was markedly higher.

4.3. Porosimetry

Cumulative pore volume included both pores and cracks; it was determined on samples matured for 28 days at 20°C. The total pore and crack volumes corresponded to the 28 day strengths, in particular to the flexural strength. The G1 mixture with the lowest flexural strength of 2.32 MPa had the largest total pore and cracks volume ($0.169 \text{ cm}^3 \cdot \text{g}^{-1}$).

On the other hand, the G5 mixture with a 5.28 MPa flexural strength had a total pore and crack volume of $0.135 \text{ cm}^3 \cdot \text{g}^{-1}$. The curves showing cumulative pore and cracks volume display specific pore diameter and crack intervals in which most of the total number of pores and cracks in all specimens are present. The G1 mixture had a range of pore diameters from 0.25 to $0.03 \mu\text{m}$, G3 had diameters of 0.15 to $0.03 \mu\text{m}$, and the G5 mixture had 1 to $0.1 \mu\text{m}$. Sample G5 contained larger pores and cracks, but their cumulative volume was lower than in the case of samples G1 and G3 (Figure 6).

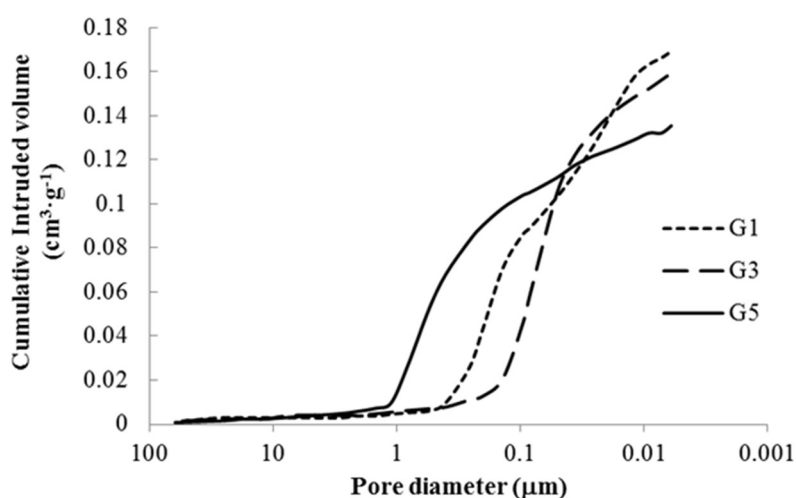


Figure 6. Cumulative volume of pores.

4. 4. Microstructure

Micrographs of samples G1, G3 and G5 matured for 28 days at 20°C are present in Figures 7–9. Sample G1 contained grains below 90 μm in size and this led to the formation of a compact binder. The pores in the binder were very small but the binder's compactness was broken by the formation of shrinkage cracks. The G3 sample had fewer shrinkage cracks, and the G5 sample had the fewest. The larger grains located in the binder perform the function of an aggregate that transmits the stress resulting from the shrinkage of the binder phase. The micrographs verify the results of the porosimetry measurements.

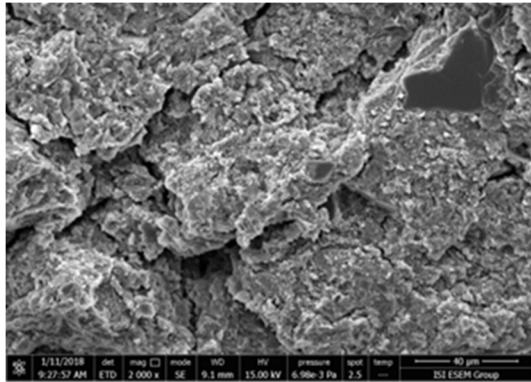


Figure 7. Sample G1.

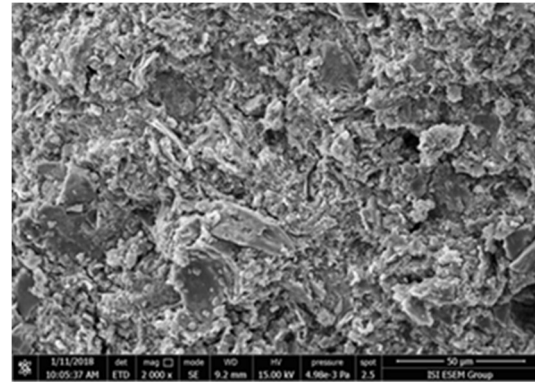


Figure 8. Sample G3.

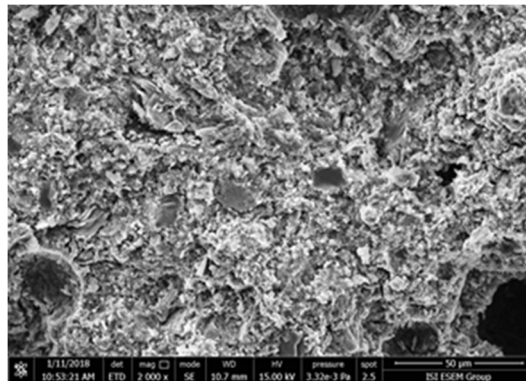


Figure 9. Sample G5.

5. Conclusions

This paper has focused on the properties of fresh and hardened alkali-activated brick powder pastes in connection with the grain size of the powder. The main conclusions are as follows:

- The pastes were shear-thickening suspensions with very high yield stress and low viscosity; the paste structure became less stiff with increasing particle size of brick powder.
- The flexural strength of samples cured at a temperature of 20°C increased over time and with increasing brick dust grain size.
- The compressive strength increased depending on the grain size of the brick powder up to 28 days; the strengths of all samples were similar after 90 days.
- Both of the strengths of the samples treated at 65°C were significantly higher.
- The mixtures prepared with the smallest grain size of brick powder showed the largest total pore and cracks volume. The high value of pore and crack volume is due to formation of shrinkage cracks.

- The compactness of the binder and significant shrinkage cracks decreasing with grain size of brick powder.
- The porosimetry measurements, tensile strengths and microstructure images were mutually consistent.

Acknowledgments

This research has been supported by the Czech Science Foundation under project No 16-02862S.

References

- [1] Reig L, Soriano L, Borrachero M V, Monzó J and Payá J 2013 *Constr. Build. Mater.* **43** pp 98–106
- [2] Robayo R A, Mulford A, Munera J and Mejía de Gutiérrez M 2016 *Constr. Build. Mater.* **128** pp 163–9
- [3] Komnitsas K, Zaharaki D, Vlachou A, Bartzas G and Galetakis M 2015 *Adv. Pow. Tech.* **26** pp 168–186
- [4] Sassoni S, Pahlavan P, Franzoni E and Bignozzi M C 2016 *Ceram. Int.* **42** pp 14685–14694
- [5] Louati S, Baklouti S and Samet B 2016 *Appl. Clay Sci.* **132-133** pp 571–8
- [6] Puertas F, Varga C and Alonso M M 2014 *Cem. Concr. Comp.* **53** pp 279–288
- [7] Singh B, Ishwarya G, Gupta M and Bhattacharyya S K 2015 *Constr. Build. Mater.* **85** pp 78–90
- [8] Kashani A, Provis J L, Qiaoa G G and van Deventer J S J 2014 *Constr. Build. Mater.* **65** pp 583–591
- [9] Favier A, Habert G and de Lacaillerie J B E 2013 *Cem. Concr. Res.* **48** pp 9–16
- [10] Mezger T G 2014 *The Rheology Handbook* 4th ed. (Hannover: Vincentz Network)
- [11] Navrátilová E and Neděla V 2016 *Microsc. Microanal.* **22** (S3) pp 1862–3
- [12] Navrátilová E and Neděla V 2017 *Microsc. Microanal.* **23** (S1) pp 2186–7
- [13] Poulesquen A, Frizon F and Lambertin D 2011 *J. Non-Cryst. Solids.* **357** pp 3565–3571
- [14] Aboulayt A, Riahi M, Anis S, Ouazzani T M and Moussa R 2014 *Int. J. Innov. Appl. Stud.* **7** pp 1170–7